A New CsI(undoped) Endcap Photon Veto System for BNL E787: A Study of the Decay $K^+ \to \pi^+\nu\bar{\nu}$

I-H.Chiang[(1)], E.Garber[(1)], T.Inagaki[(2)], K.Ino[(3)], S.Kabe[(2)], S.Kettell[(1)], M.Kobayashi[(2)], T.K.Komatsubara[(3)], Y.Kuno[(2)], K.K.Li[(1)], L.S.Littenberg[(1)], T.Morimoto[(3)], T.Nakano[(4)], K.Omata[(3)], T.Sato[(2)], T.Shinkawa[(2)], S.Sugimoto[(3)], K.Tauchi[(3)], A.Yamashita[(1)] and Y.Yoshimura[(2)]

[(1)]*Brookhaven National Laboratory (BNL), Upton, NY 11973*

[(2)]*National Laboratory for High Energy Physics (KEK), Tsukuba 305, Japan*

[(3)]*Institute for Nuclear Study (INS), University of Tokyo, Tokyo 188, Japan*

[(4)]*Osaka University, Osaka 560, Japan*

ABSTRACT

A new CsI(undoped) calorimeter has been installed for the endcap photon veto system of BNL E787, a search for the decay $K^+ \to \pi^+\nu\bar{\nu}$. This new endcap provides substantially more light output than the previous Pb-scintillator endcap and has better timing resolution.

1. Introduction

The experiment E787[*] at the Alternating Gradient Synchrotron (AGS) at BNL is searching for the decay $K^+ \to \pi^+\nu\bar{\nu}$[1]. The standard model predicts this branching ratio to occur at $\sim 10^{-10}$. A measurement of this branching ratio is particularly interesting, as it is sensitive to the CKM matrix element V_{td} and the theoretical uncertainties are not very large ($\sim$7%) [2].

The signature for the decay $K^+ \to \pi^+\nu\bar{\nu}$ is a single charged pion track, so a search for this decay at a sensitivity of $\sim 10^{-10}$ requires a very efficient veto of the photons from the copious $K^+ \to \pi^+\pi^\circ$ ($K_{\pi2}$) decay, a large rejection of muon tracks by requiring the observation of the decay chain $\pi^+ \to \mu^+ \to e^+$, and good reconstruction of the energy, range and momentum of the charged track .

The two π° photons from $K_{\pi2}$ decay at rest have energies between 20–225 MeV, but due to unavoidable gaps and dead material in the detector it is necessary to veto energy deposits of even lower energy. Essentially, the whole E787 detector is used to veto photons. The photon veto has to be efficient in the very high rate environment necessary to measure a 10^{-10} branching ratio, yet not introduce a large inefficiency caused by accidental vetoing of good events. This requires good timing resolution in almost all detector systems.

A diagram of the E787 detector is shown in figure 1. The previous version of the detector has been described elsewhere[3]. The new endcap system is described below.

[*]E787 collaboration: BNL, Princeton University, TRIUMF, KEK, INS and Osaka University

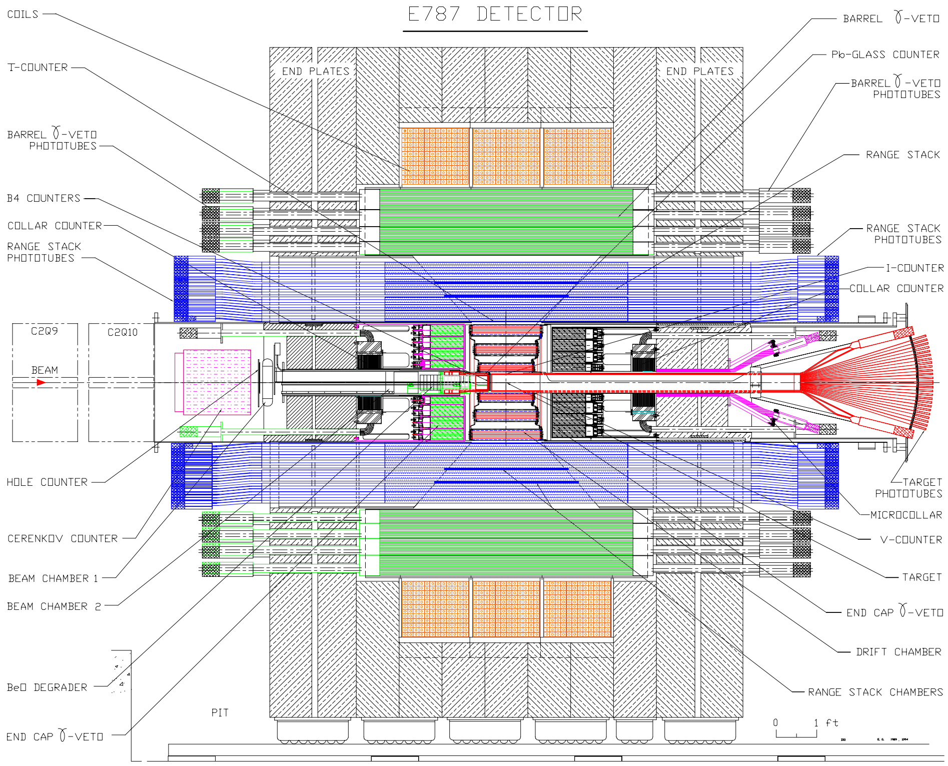

Figure 1: The E787 detector.

2. CsI Endcap Photon Veto System

The endcap is in a particularly high rate environment near the beam. The old endcap was constructed as a Pb-scintillator sandwich with a visible energy/ deposited energy of 30%. The light output was only a couple of photoelectrons per MeV of deposited energy (pe/MeV) and the timing resolution for 3 MeV photons was greater than 2.5 ns. In addition, due to the large amount of dead material (Pb) the old endcap was more likely miss photons that underwent photonuclear interactions.

The width of the veto window should be as narrow as possible to reduce losses from accidental hits. It is also necessary to be efficient for detecting signals riding on the tails of earlier hits. The CsI provides substantially more light than the old endcaps and should provide much better timing resolution, but since it is slower, pulse recognition of signals on the tails of earlier signals is more difficult. The slow component of scintillation light is suppressed through the use of optical filters and the pulses are recorded with transient digitizers to obtain good rejection of overlapping signals. The design of the endcap is to achieve sub-nanosecond timing resolution for 1 MeV signals.

2.1. CsI Crystals

The endcaps consist of 143 CsI(undoped) crystals arranged in four concentric rings in each endcap (75 crystals in the upstream endcap and 68 crystals in the downstream endcap). The crystals are right-pentagonal-polyhedrons (see figure 2a). The dimensions of the Ring 1 crystals are A=7.8–8.0 cm, B=6.1 cm and C=25.0 cm; the dimensions of the Ring 2–4 crystals are A=9.9–11.2 cm, B=8.6 cm and C=25.0 cm. They were grown by Crismatec using the Kyropoulos method. The ingots were 16"–19" in diameter and needed to be greater than 4" high in order to cut crystals for Ring 2–4. The number of Ring 2–4 crystals cut from one ingot varied from 1–3. These large crystals generally have good light output, a mean of 255 pe/MeV for full photocathode coverage (QE=16%).

CsI is a dense scintillator that is relatively fast with reasonably good light output. [4] The density is $\rho = 4.5$ g/cm^3; the radiation length is $\chi_0 = 1.86$ cm; the Moliere radius is $R_M = 3.8$ cm. Undoped CsI has at least two components of scintillation light, the fast component has a time constant of $\sim$45 ns and the slow component has a time constant of $\sim$600 ns. The time constant of the fast component measured with these large crystals is slightly larger than for smaller crystals. The fast component has a peak emission at $\sim$310 nm, while the slow component peaks at $\sim$450 nm. The ratio of fast to slow components is a measure of the quality of the crystal and is frequently quoted as F/T, where F (Fast) is the integrated charge in a 100 ns ADC gate and T (Total) is the integrated charge in a 1 μs gate. The crystal light output and F/T ratio are shown in figure 2(b). The light output is measured with a 5" PMT with a UV glass window. With this PMT the entire crystal surface is covered by the photocathode and the measured light yield varies from 180–310 pe/MeV. There is a strong correlation between F/T and npe/MeV.

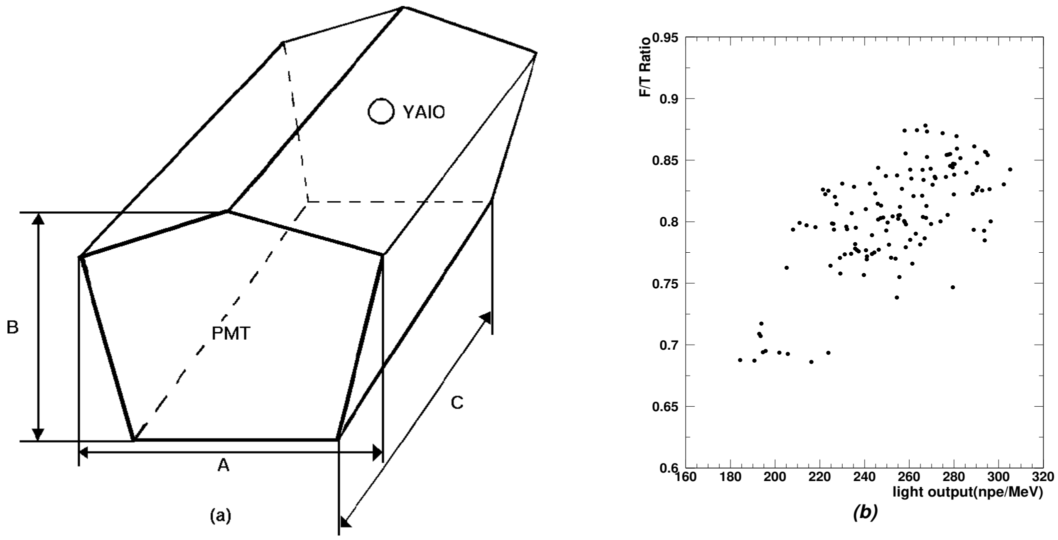

Figure 2: (a) Sketch of CsI crystal. (b) Plot of the F/T ratio vs the crystal output (for full PMT coverage).

The crystal size and shape were designed minimize the amount of dead material in the endcap. Each crystal is wrapped with 0.008" Teflon (in 3 layers) and 0.0015"

Al-Mylar. This assembly is then wrapped with 0.0015" Monokote to protect the inner wrapping and to provide optical isolation. Increasing the Teflon beyond 0.008" increases the light yield only slightly, while adding more dead material. The open end of each crystal has a white Noryl flange (with holes for the PMT and for a quartz optical fiber) glued to it with a whitened epoxy (Stycast 1266 with MgO, 1:1 by weight). The white flange and white epoxy were found to increase the light output by about 15% relative to a black flange with clear epoxy. This flange is used to mount the PMT to the crystal and the crystals onto the aluminum support plate of the endcap. The material between the crystals and the target has been minimized — only the wrapping and a 0.188" lucite endplate (the inner wall of the endcap, inside of Ring 1, is 0.031" Al). The lucite cover helps to provide a seal of the crystal volume; dry nitrogen is continuously flowed into the endcap to keep the humidity low (5-15%).

2.2. High Field Fine-Mesh Phototubes

The PMTs are directly coupled to the crystals in order to maximize the light collection, so they must operate with high gain in a 10 kG magnetic field. They must have high quantum efficiency (QE) at a wavelength of 310 nm (need UV glass or quartz window) and large photocathode area. Fine-Mesh PMTs were designed for this experiment by Hamamatsu. They are high gain, 19-stage PMTs with 14.5 cm^2 (2" PMT) and 32.2 cm^2 (3" PMT) photocathodes and UV glass windows. The gain is greater than 2×10^7 at $\mathbf{B}$=0 kG, with typical gains of $1\text{–}2{\times}10^6$ at 9.6 kG. The gain drop in the E787 detector is $\sim$ 40, at $\mathbf{B}$=9.6 kG. They have reasonably fast rise times, high QE (average QE=17%), but not very good single photoelectron resolution. The ring 1 crystals use 2" PMTs (R4721mod) and the larger crystals use 3" PMTs (R5065mod).

Each PMT has an Kenko U330 filter glued onto it. The PMT/filter combination then has a 3 mm thick cookie of Sylgard 527 silicone gel formed onto it. The surface is slightly convex, to allow good optical coupling to the crystal and to allow for removal of the PMT from the crystal. The F/T ratio is typically 80% without the filters and 86% with the filters. There is a loss of $\sim$15% of the fast light and a suppression of the slow component by almost an order of magnitude with the filter.

The PMTs are mounted to the crystals with a spring loaded locking mechanism that keeps a constant pressure of 7 pounds on the cookie.

2.3. Electronics

Signals from the CsI PMTs are amplified (PS776 $\times$10 amplifiers) and then split three ways (0.5:0.4:0.1). The first output goes to an 8-bit, 500 MHz (256 ns range) CCD transient digitizer[5] for pulse recognition and precise timing, the second output goes to a 11 bit ADC (LRS4300B) for energy calibration, and the third output is multiplexed by four and is then sent to a high range ADC, a high-range CCD and to a discriminator. The discriminator output is used for the photon veto requirement of the L0 trigger. The discriminated signal is also sent to a 1 ns least count, (2μs range) TDC (LRS1789) as a check on the CCDs and for measuring rates. The high-range ADC and CCD are used due to the large dynamic range of the photons of interest.

An average pulse shape from the CCDs is shown for one of the crystals in figure 3(a). (The signal has been delayed with 250 ns of RG8x cable and 150 ns of RG58 cable.) A fit to the pulse shape is overlayed on the histogram, the rise time is 9.9 ns and the fall time is 44.1 ns.

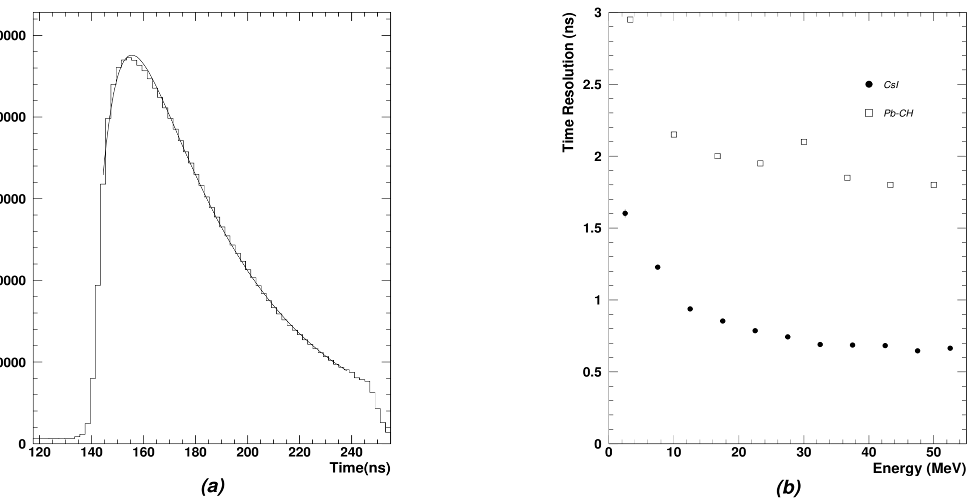

Figure 3: (a) An average pulse shape in the low-range CCD for one crystal. (b) Timing resolution for old and new endcaps as a function of energy.

2.4. Monitoring System

The PMT gain is monitored with three separate techniques 1) a Xe lamp , 2) $YAlO_3$:Ce(^{241}Am) light pulsers[6], and 3) calibration triggers from $K^+ \rightarrow \mu^+\nu$ ($K_{\mu 2}$) decays. The Xe lamp (Hamamatsu L2436) output is monitored by 2 PIN photodiodes and the light is distributed by quartz fibers to all 143 crystals and several reference PMTs. The Xe light is broad band the spectrum is cut by a UV filter to match the light spectrum of CsI scintillation; the pulse width (FWHM$\sim$120ns) is considerably longer than that of the CsI (FWHM$\sim$35ns), but has been shown to be stable over time. The resolution is 2–3%. Over the one month of running the Xe light output was stable to $\pm$0.4%. Both the Xe lamp and reference PMTs are in temperature controlled environments. These temperatures, as well as the temperatures of the crystal and PMT environments, are monitored once per AGS spill (every 4 seconds). The Xe lamp is triggered by a clock synchronized to the AGS RF to flash once between each AGS spill. This provides a continual monitoring of the PMT gains.

The YAlO light pulsers are glued to the CsI crystal on the end facing the PMT. They scintillate at a wavelength that is well matched to the CsI and have a similar pulse shape (FWHM$\sim$50 ns). They are calibrated to the ^{137}Cs peak between AGS runs; their typical equivalent energy is 4–9 MeV. Special runs, triggering on the YAlO signals, are made to set the PMT HV and then about once per week as an additional check of the gain calibration.

The energy calibration is accomplished by comparing the energy deposited by muons from $K_{\mu 2}$ decays in data and Monte Carlo simulations. The $K_{\mu 2}$ muons are mono-energetic (152 MeV) and, neglecting corner clipping, stop in the CsI; however, due to the variation in kaon stopping position in the target, the peak is quite broad. Special triggers are made with $K_{\mu 2}$ decays with the muon stopping in the endcap. These calibration triggers are accumulated continuously with the $\pi\nu\bar{\nu}$ data, and special calibration runs are made every few weeks. This energy calibration is verified by reconstructing the π° from $K_{\pi 2}$ decays, where one photon converts in the barrel veto and one converts in the endcap. The current level of agreement is better than 10%.

The timing calibration is done by comparing the time of photons in the endcap with the π^+ in the range stack from $K_{\pi 2}$ decays.

3. Initial Performance

The new CsI endcap calorimeter was installed for the 1994 AGS run. Data on the performance has been collected and analyzed and some preliminary results have been obtained.

Rates are measured by counting random hits in the TDCs (for energies above $\sim$10 MeV) and from special runs where a small number of endcap crystal signals were sent to the long baseline Transient Digitizers [7] (500MHz, 8 bit, 6μs range). The rates in the inner rings (Ring 1–2) on the upstream endcap are quite high. The number of kaons entering the target (K_B) has been raised from K_B=300 k/spill (the effective AGS spill length is $\sim$ 0.8–1 sec) to K_B=1.2 M/spill, with the goal to reach K_B=3 M/spill. With K_B=1.2 M/spill, the incident kaon rate measured at the beam Cherenkov counter is C_K=6 M/spill and the incident pion rate is C_π=1.5 M/spill. At this intensity the rate per crystal (2 MeV threshold) in the upstream endcap Ring 1 is 850 kHz; Ring 2 is 650 kHz, and the other Rings (including downstream) vary from 150–250 kHz. The rate (R) dependence on energy threshold (E) is fit with a sum of two exponentials

$$R(E) = A_1 e^{-E/E_1} + A_2 e^{-E/E_2} \tag{1}$$

with E_2=40 MeV and 1.3 MeV< E_1 <3.5 MeV. The total rate in the upstream endcap is estimated to be 15.4†(3.6) MHz with a 2 MeV(30 MeV) threshold. The fraction of endcap hits above 30 MeV which are in coincidence with C_K is 76% and the fraction in coincidence with C_π is 17%. The total rate in the downstream endcap is 50%(60%) of the upstream endcap. The average number of crystals hit per event is 2 (for thresholds above 5 MeV).

The calibration of the detector is continuing, but some preliminary results on the endcap timing show that the resolution is less than 1 ns for all $K_{\pi 2}$ decays. The timing resolution as a function of photon energy is shown in figure 3(b). We see that for energies above 10 MeV the resolution is better than 1 ns and at all energies we

†assuming a multiplicity of 2

have 2–3 times better resolution than with the old endcap. We expect even further improvements as the calibrations are refined.

4. Conclusions

Two new photon veto endcaps using undoped CsI crystals have been constructed and installed into the E787 detector. We have measured an improvement of a factor of 2–3 in the endcap time resolution. Further improvements are expected. Calibration of the detector is continuing and a measurement of the veto efficiency for $K_{\pi 2}$ photons should be available soon.

5. Acknowledgements

We gratefully acknowledge J.R. Cuccia Jr., W. Lenz, G. Munoz, and H. Ratzke for their valuable technical assistance. This work was supported in part by the U.S. Department of Energy, under contract number DE-AC02-76CH00016, and in part by the Ministry of Education, Science and Culture of Japan through the Japan-U.S. Cooperative Research and Development Project in Energy and Related Fields.

6. References

1. M.S. Atiya *et al.*, *Phys. Rev. Lett.* **70**(1993)2521; *Phys. Rev.* **D48**(1993)R1.
2. G. Buchalla and A. Buras, *Nucl. Phys.* **B412** (1994) 106.
3. M.S. Atiya *et al. Nucl. Instr. and Meth.* **A321** (1992) 129.
4. Z. Wei and R. Zhu, *Nucl. Instr. and Meth.* **A326** (1993) 508; C.L. Woody *et al.*, *IEEE Trans. Nucl. Sci.* **37** (1990) 492; S. Kubota *et al.*, *Nucl. Instr. and Meth.* **A268** (1988) 275.
5. D. Bryman *et al.*, *IEEE Trans. Nucl. Sci.* **38** (1991) 295.
6. M. Kobayashi *et al.*, *Nucl. Instr. and Meth.* **A337** (1994) 355.
7. M. Atiya *et al.*, *IEEE Trans. Nucl. Sci.* **36** (1989) 813; *Nucl. Instr. and Meth.* **A279** (1989) 180.